

Polymer Chemistry

Accepted Manuscript



This is an *Accepted Manuscript*, which has been through the Royal Society of Chemistry peer review process and has been accepted for publication.

Accepted Manuscripts are published online shortly after acceptance, before technical editing, formatting and proof reading. Using this free service, authors can make their results available to the community, in citable form, before we publish the edited article. We will replace this *Accepted Manuscript* with the edited and formatted *Advance Article* as soon as it is available.

You can find more information about *Accepted Manuscripts* in the [Information for Authors](#).

Please note that technical editing may introduce minor changes to the text and/or graphics, which may alter content. The journal's standard [Terms & Conditions](#) and the [Ethical guidelines](#) still apply. In no event shall the Royal Society of Chemistry be held responsible for any errors or omissions in this *Accepted Manuscript* or any consequences arising from the use of any information it contains.



Journal Name

ARTICLE

Smart Block Copolymers of PVP and an Alkylated PVP Derivative: Synthesis, Characterization, Thermoresponsive Behaviour and Self-assembly

Received 00th January 20xx,
Accepted 00th January 20xx

DOI: 10.1039/x0xx00000x

www.rsc.org/

Johnel Giliomee, Rueben Pfukwa, Nonjabulo P. Gule, Bert Klumperman*

Stimuli responsive block copolymers of biocompatible poly(3-ethyl-*N*-vinylpyrrolidone) and poly(*N*-vinylpyrrolidone), i.e. EPVP-PVP, were readily synthesized via RAFT-mediated polymerization. The thermoresponsive behaviour and temperature induced self-assembly, in aqueous solutions, was studied using various spectroscopic and microscopic techniques. We obtained different morphologies, i.e. spherical and cylindrical micelles, and vesicles, via temperature induced self-assembly, of aqueous solutions of a single diblock copolymer by simply adjusting the solution concentration. This study establishes the biocompatible EPVP/PVP combination as a versatile stimuli responsive block copolymer system suitable for applications in drug delivery.

Introduction

Thermoresponsive polymers exhibit reversible phase transitions in response to temperature changes, making them particularly well suited for nanotechnological and biomedical applications.¹⁻⁴ Polymers displaying a lower critical solution temperature (LCST) are particularly popular. Such polymers are soluble in water below the cloud point temperature (T_{CP}), and a sharp increase in the solution turbidity is usually observed when the phase transition takes place. The thermoresponsive behaviour is dependent on certain parameters such as concentration, molecular weight and copolymer composition.⁵⁻¹⁴ The thermoresponsive character has been incorporated into smart responsive block copolymer (BCP) systems, which typically combine a stimuli responsive block and a non-stimuli responsive segment. For BCPs, changes in intermolecular interactions, hydrophobicity or solubility in one or more of the block segments can cause drastic changes in terms of their self-assembly. These types of systems are particularly useful for controlled drug release, in self-assembled polymer therapeutics, such as micelles and vesicles.¹⁵⁻¹⁸

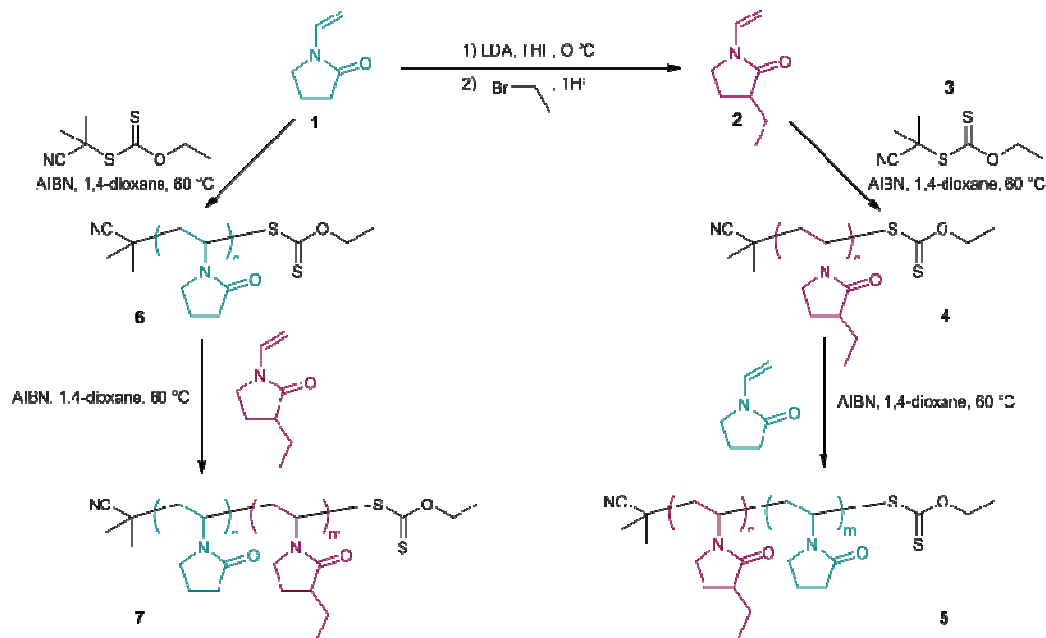
Polymer classes that display LCST behaviour include acrylamide based polymers,¹⁰ certain methacrylamino functional polymers,¹⁹ poly(2-hydroxyethyl methacrylate),²⁰ oligo(ethylene glycol) functional (meth)acrylates (OEGMA)s,^{21,22} Pluronics,^{23,24} poly(vinyl ethers),²⁵ to name a few.^{25,26} Polymers of 3-alkyl-*N*-vinylpyrrolidone are a recent addition to this family of thermoresponsive polymers,²⁷⁻²⁹ in particular poly(3-ethyl-*N*-vinylpyrrolidone) (EPVP) has been shown to have a sharp LCST at 26–27 °C.^{27,28} Alkylated

derivatives of poly(*N*-vinylpyrrolidone) (PVP) have also been shown to have a low cytotoxicity, similar to PVP, and therefore have significant potential for bioapplications.²⁹ The thermoresponsive properties of EPVP are close to physiological conditions, which puts it in the same league as other, extensively studied, thermoresponsive polymers such as poly(*N*-isopropyl acrylamide) (PNIPAM) and poly(OEGMA)s.^{2, 22, 30} Only a few studies on EPVP have been reported, and these studies largely focus on the random copolymers of alkylated PVP derivatives.^{27-29,31} Studies utilizing EPVP synthesized by reversible deactivation radical polymerization (RDRP) techniques are even fewer.³² To the best of our knowledge there are no reported examples of stimuli responsive block copolymers of 3-ethyl-*N*-vinyl pyrrolidone (ENVP), which form well defined aggregates. This interests us because PVP-based polymers, due to their excellent biocompatibility, have extensive applications in pharmaceuticals, cosmetics and food.³³ Native PVP does not display LCST behaviour below 100 °C, due to its high hydrophilicity; LCST behaviour is only induced by manipulating the polymer composition,^{27,34} or in the presence of additives.³⁵⁻³⁸

In this work we describe thermoresponsive BCPs based on EPVP-*block*-PVP (EPVP-PVP), and PVP-*block*-EPVP (PVP-EPVP) synthesized by the reversible addition fragmentation chain transfer (RAFT) polymerization technique, using xanthate chain transfer agents (Scheme 1). The propagating radicals of ENVP and *N*-vinylpyrrolidone (NVP) are essentially identical, therefore the two block segments can be readily synthesized in any order without restrictions imposed by the leaving group abilities of the macro-RAFT agent (i.e. first block segment) and the second block's monomer.³⁹ These BCPs display reversible temperature dependent aqueous solubility. We also show the (concentration dependent) formation of well-defined aggregates i.e. spherical micelles, cylindrical micelles and vesicles.

* Department of Chemistry and Polymer Science, Stellenbosch University, Private Bag X1, Matieland 7602, South Africa

Electronic Supplementary Information (ESI) available: [details of any supplementary information available should be included here]. See DOI: 10.1039/x0xx00000x



Scheme 1. Synthesis of EPVP and PVP based block copolymers

Experimental

Materials and methods. All chemicals and solvents were purchased from commercial sources and used without further purification, unless stated otherwise. NVP (Aldrich, 99%) was purified by distillation under reduced pressure, and kept over molecular sieves. Tetrahydrofuran (THF) was distilled over sodium/benzophenone ketyl. AIBN (Riedel de Haen) was recrystallized from methanol. Moisture and oxygen sensitive reactions were carried out under an inert atmosphere using argon gas. All compounds were characterized by NMR spectroscopy using a Varian VXR-Unity (300 MHz or 400 MHz) spectrometer. Samples were dissolved in deuterated solvents and chemical shifts are reported in parts per million (ppm), where tetramethylsilane (TMS) was used as internal reference. Variable temperature (VT) ^1H NMR spectra were recorded on samples dissolved in D_2O and CDCl_3 , respectively, at a concentration of 5 mg/mL. At each temperature step (2 °C) from 20 °C to 40 °C, the samples were equilibrated before the measurement was taken. The apparent EPVP to PVP ratio was determined from the integrated ethyl ($-\text{CH}_3$) signal from E-PVP and the combined EPVP and PVP signals, as demonstrated in text.

Size exclusion chromatography (SEC) was measured on a system equipped with a Shimadzu LC-10AT isocratic pump, a Waters 717+ autosampler, a column system fitted with a PSS guard column (50 × 8 mm) in series with three PSS GRAM columns (300 × 8 mm, 10 μm , 2 × 3000 Å and 1 × 100 Å) kept at 40 °C, a Waters 2487 dual wavelength UV detector and a Waters 2414 differential refractive index (DRI) detector. Dimethylacetamide (DMAc) was used as the eluent, stabilized with 0.05 % BHT (w/v) and 0.03 % LiCl (w/v), at a

flow rate of 1 mL.min $^{-1}$. Prior to analysis, polymer samples were filtered through 0.45 μm GHP filters. The molar masses of polymers were calculated against poly(methyl methacrylate) (PMMA) standards (Polymer Laboratories) ranging from 690 to 1.2×10^6 g.mol $^{-1}$.

Turbidimetry. Turbidity measurements were performed on a Perkin Elmer Lambda 20 photodiode array spectrophotometer, consisting of a holographic monochromator, pre-aligned deuterium and halogen lamps and a photodiode array detector. A temperature controller was connected and in-cell measurements of the temperature were taken. The sample concentrations were kept constant at 1 mg.mL $^{-1}$, unless stated otherwise. The transmittance at 500 nm was monitored and the data were collected at 20 °C to 50 °C with 1 °C increments. An equilibration time of 30 min was allowed prior to each measurement. The cloud point temperatures (T_{CP}) were determined as the temperature where the transmittance is 50 % of the initial transmittance.

Dynamic light scattering (DLS). DLS was performed on a ZetaSizer 1000 HS $_z$ (Malvern Instruments, Malvern) equipped with a 4 mW He-Ne laser, operating at a wavelength of 633.0 nm and a scattering angle of 90 °. Sample concentrations were kept constant at 1 mg.mL $^{-1}$. Samples were heated from 20 °C to 50 °C in 2 °C steps. At each temperature step, the samples were equilibrated for 300 s and then measured three times. Each measurement comprised of 10-15 sub-runs to determine the particle sizes. The intensity distribution of the particle sizes was then calculated using CONTIN analysis.

Transmission electron microscopy (TEM) and cryogenic transmission electronic microscopy (cryo-TEM).

TEM was performed on a FEI Tecnai G2 20 TWIN with a Gatan Tridiem 863 energy filter, incorporating a built-in CCD camera

microscope, operating with an accelerating voltage of 120 kV. The samples were prepared on a plasma treated carbon-coated copper grid and stained with uranyl acetate. Samples of 3 mg.mL⁻¹ were either cooled to 5 °C (for measurements below the LCST) or manually heated from 20 °C to 37 °C at a heating rate of 1 °C.min⁻¹ (for measurements above the LCST). TEM samples for the studies on the effect of concentration on morphology were prepared in a similar manner, representative sample loadings include 70 mg.mL⁻¹ (for 7 weight %), 110 mg.mL⁻¹ (for 11 weight %) and 180 mg.mL⁻¹ (for 18 weight %).

Cryo-TEM measurements were performed on a FEI Tecnai F20 CRYO FEGTEM operating at an acceleration voltage of 120 kV. Images were recorded with a bottom mounted 1 k × 1 k CCD camera. A sample concentration of 3 mg.mL⁻¹ was used. A drop of the polymer solution was rapidly placed on a perforated carbon grid and 2 min equilibration time was allowed. The samples were then rapidly plunged into a cryogen reservoir containing liquid ethane. After preparation, the samples were stored and measured at a temperature below -179 °C.

Monomer and RAFT agent synthesis. The monomer, ENVP,²⁷ and xanthate chain-transfer agent (CTA), *S*-(2-cyano-2-propyl) *O*-ethyl xanthate,⁴⁰ were synthesized according to reported procedures.

Synthesis of EPVP or PVP macro-RAFT agents. A typical procedure for the RAFT mediated polymerizations of NVP and ENVP is

described, using ENVP as an example. Variations in target degree of polymerization (DP) are given in Table 1.

ENVP (1.00 g, 7.18 mmol), xanthate CTA (**3**) (19.4 mg, 0.10 mmol) and AIBN (0.0034 g, 0.02 mmol) were dissolved in dioxane (0.5 g) and placed in a 10 mL pear-shaped flask. The reaction mixture was degassed by purging with argon for 1 h, after which it was immersed in an oil bath preheated at 60 °C. The reaction proceeded by stirring for 24 h. EPVP was isolated by precipitation in pentane.

Synthesis of block copolymers, EPVP-PVP and PVP-EPVP. A typical procedure for the RAFT-mediated block polymerizations of EPVP with PVP, and PVP with EPVP is given below, using EPVP-PVP as an example. Variations in target DP of the blocks, and block sequence, are given in Table 2.

EPVP macro-RAFT agent, EPVP-2 (0.20 g, 0.025 mmol), NVP (0.11 g, 1.0 mmol) and AIBN (0.8 mg, 0.005 mmol) were dissolved in dioxane (0.5 g) and placed in a 10 mL pear-shaped flask. The reaction mixture was degassed by purging with argon for 1 h, after which it was immersed in an oil bath preheated at 60 °C. The reaction proceeded by stirring 24 h. The block copolymers were isolated by precipitation from pentane and further purified via dialysis against distilled water. Subsequent freeze-drying afforded the block copolymer, BCP-3.

Table 1. RAFT mediated polymerization of ENVP and NVP.

| label | Monomer. | Target DP | α^a | $M_{n, \text{theoretical}}$ (g/mol) | $M_{n, \text{NMR}}^b$ (g/mol) | $M_{n, \text{SEC}}^c$ (g/mol) | \bar{D}^d | % chain end loss ^e |
|--------|----------|-----------|------------|-------------------------------------|-------------------------------|-------------------------------|-------------|-------------------------------|
| EPVP-1 | ENVP | 70 | 50% | 5000 | 5700 | 4200 | 1.25 | 19 |
| EPVP-2 | ENVP | 70 | 80% | 7900 | 8100 | 8000 | 1.28 | 10 |
| EPVP-3 | ENVP | 140 | 60% | 11800 | 18500 | 12600 | 1.40 | 28 |
| PVP-1 | NVP | 45 | 65% | 3400 | 3500 | 3700 | 1.12 | 11 |

^aConversion determined from ¹H NMR spectroscopy. ^b $M_{n, \text{NMR}}$ determined from ¹H NMR spectroscopy. ^c $M_{n, \text{SEC}}$ and ^ddispersity obtained from SEC in DMAC relative to PMMA standards. ^eThe percentage unsaturated chain-ends as calculated from ¹H NMR spectroscopy. All polymerizations were run for 24 h.

Table 2. Block copolymer synthesis.

| label | Macro RAFT agent | Target M_n | $M_{n, \text{SEC}}^a$ (g/mol) | Copolymer Composition ^b | Molar Ratio ^c (EPVP:PVP) | f_{phil}^d | \bar{D} |
|-------|------------------|--------------|-------------------------------|---|-------------------------------------|---------------------|-----------|
| BCP-1 | EPVP-1 | 6000 | 4900 | EPVP ₃₀ - <i>b</i> -PVP ₆ | 80:20 | 15% | 1.33 |
| BCP-2 | | 11000 | 10900 | EPVP ₅₈ - <i>b</i> -PVP ₂₆ | 73:27 | 26% | 1.40 |
| BCP-3 | EPVP-2 | 12500 | 12200 | EPVP ₅₈ - <i>b</i> -PVP ₃₈ | 62:38 | 34% | 1.45 |
| BCP-4 | | 14500 | 14400 | EPVP ₅₈ - <i>b</i> -PVP ₅₆ | 59:41 | 43% | 1.38 |
| BCP-5 | EPVP-3 | 25000 | 25500 | EPVP ₉₀ - <i>b</i> -PVP ₁₁₆ | 48:52 | 50% | 1.67 |
| BCP-6 | PVP-1 | 10000 | 8100 | PVP ₃₂ - <i>b</i> -EPVP ₃₁ | 46:54 | 54% | 1.54 |

^a $M_{n, \text{SEC}}$ obtained from SEC in DMAC based on PMMA standards. ^bDetermined from $M_{n, \text{SEC}}$ of homopolymers and block copolymers. ^cRatios calculated from ¹H NMR spectroscopy by integrating signals of EPVP and the combined signals of EPVP and PVP. ^dHydrophilic mass fraction, f_{phil} calculated from M_n , copolymer composition.

Results and discussion

Homo and block copolymer synthesis and characterization. EPVP is a relatively new thermoresponsive polymer, which displays LCST behaviour close to physiological conditions.²⁷ The structural

similarity between ENVP and NVP suggested that ENVP synthesized could be polymerized via the RAFT technique, using xanthate chain transfer agents, such as *S*-(2-cyano-2-propyl) *O*-ethyl xanthate, as with NVP homopolymerizations.⁴¹ We studied the RAFT polymerization of ENVP, using xanthate chain transfer agents to allow for comparison with NVP. M_n increased linearly as a function

of increasing conversion, supporting the livingness of the polymerization system (Fig. 1a). The discrepancy between theoretical and experimental M_n values (Fig. 1a) was attributed to the use of PMMA standards in the SEC calibration. The \mathcal{D} values obtained by analyzing the polymers at different conversion values, were consistently low, $\mathcal{D} < 1.4$ (Fig. 1a), and the SEC traces were monomodal (Fig. 1b and c), typical of a well behaved RAFT-mediated polymerization. Different molar mass EPVP homopolymers were then synthesized, to act as macro-RAFT agents for subsequent chain extension with NVP (Table 1). Conversion values, however, were not consistent, even under similar reaction conditions. The monomer NVP (reversibly) forms a number of side products, in the presence of water (even very small amounts). The variable occurrence of this phenomenon, in different polymerizations, although it does not affect the RAFT mechanism, lowers the reproducibility of final conversions, in the RAFT mediated polymerization of NVP.⁴² Due to the structural similarity between NVP and ENVP, it is likely that a similar phenomenon is also at play. Additionally, we observed that the xanthate ω -chain ends were labile, even at relatively low reaction temperatures, of 60 °C, resulting in the formation of unsaturated chain ends (Fig. 2, and Scheme 2), up to 10-30%. These peculiarities are consistent with observations during the xanthate mediated RAFT polymerization of NVP.⁴² Nonetheless \mathcal{D} values were reasonably low. We also synthesized a well-defined PVP homopolymer to use as macro-RAFT agents for subsequent chain extension with ENVP.

BCPs were synthesized by chain extending from either EPVP or PVP, with NVP or ENVP, respectively. We targeted various block ratios of EPVP:PVP, with hydrophilic mass fractions, f_{phil} ranging from 15 % to 50% (Table 2), in order to assess the effect on the temperature responsive behaviour and the morphology of the self-assembled aggregates. We confirmed the successful synthesis of the BCPs by SEC and ¹H NMR spectroscopic analysis. With the former technique, SEC traces shifted to lower elution volumes, consistent with an increasing molecular weight of the polymers (Fig. 3 and Fig. S1). We observed tailing towards the low molar mass side, which we attributed to dead homopolymer impurities carried over from the first block synthesis, as well as possible dead chains that could have formed during the chain extensions of EPVP with PVP. Nevertheless, \mathcal{D} values were reasonably low. We also evaluated the block ratios, via ¹H NMR spectroscopy, by comparing the $-\text{CH}_3$ signal, at 0.9 ppm, which is unique to ENVP to $-\text{CH}_2$ lactam and $-\text{CH}$ polymer backbone signals at 4.0 – 3.0 ppm, which are common to both ENVP and NVP (Fig. 4). The data correlated with the relative M_n values determined via SEC.

We also successfully chain extended PVP with EPVP, forming PVP-EPVP (Fig. 3b) confirming the versatility of this system. This is beneficial because there are no restrictions imposed by the leaving group ability of the macro-RAFT agent (i.e. first block segment) and the second block's monomer.³⁹

Thermoresponsive behaviour: The thermoresponsive behaviour of the various EPVP homopolymers, EPVP-PVP and PVP-EPVP BCPs was first investigated using turbidity experiments, by measuring the optical transparency at 500 nm. The cloud point temperature (T_{CP}) was taken as the temperature at which the transmittance dropped

to 50 % of its original value. Figure 5 shows the turbidimetry curves of EPVP homopolymers and the EPVP-PVP as well as PVP-EPVP block copolymers. EPVP displayed a sharp LCST at 27 °C, as

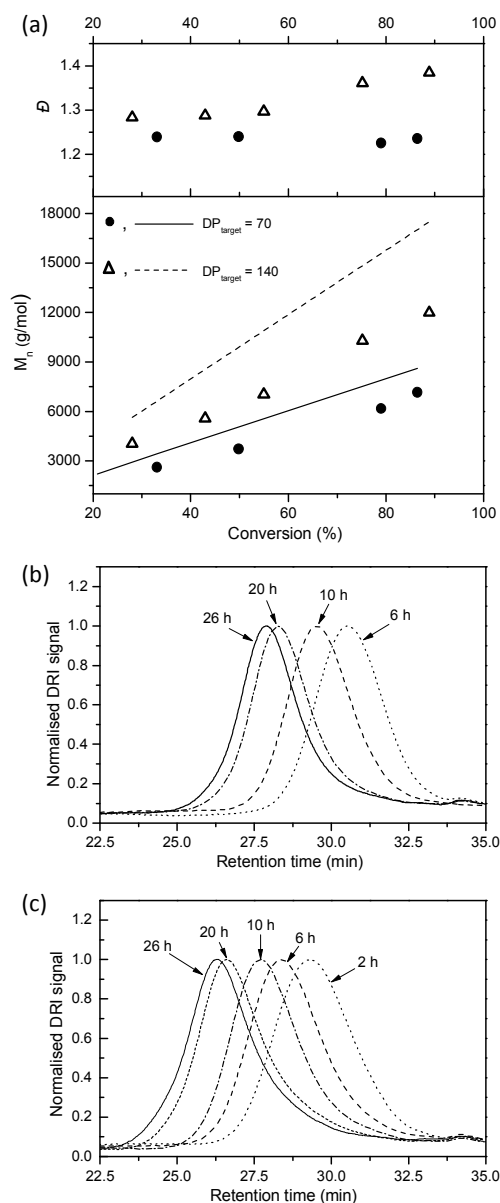


Figure 1. Evolution of M_n and \mathcal{D} (a) and the corresponding SEC traces for target $DP = 70$ (b) and 140 (c), respectively, as a function of conversion for the RAFT-mediated polymerizations of ENVP. The symbols in (a) represent \mathcal{D} and experimental M_n values, respectively, whilst the lines represent theoretical M_n values.

expected,²⁷ with solutions changing from completely clear to opaque. The BCPs showed slight changes in turbidity as the temperature was increased. It is expected that the formation of BCP aggregates will result in solubilisation of the hydrophobic blocks, therefore less dramatic changes in the turbidity of the BCP solutions were observed. As a result, the T_{CP} values were shifted to higher

temperatures (Fig. 5, Table 3, and Fig S2-S6). The initial % transmittance of the EPVP and EPVP-PVP blocks did not start at 100 % in contrast to that of the PVP-EPVP block (Fig. 5), even though all the solutions appeared completely transparent and homogenous.

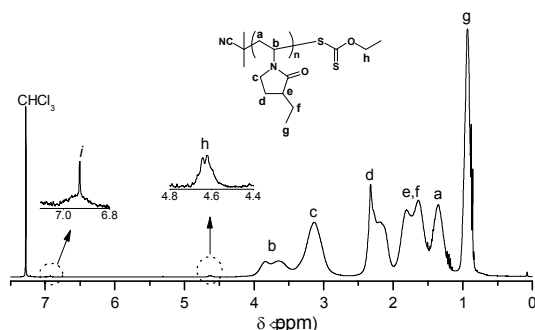
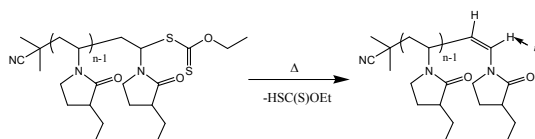


Figure 2. Representative ^1H NMR spectra of EPVP in CDCl_3 .



Scheme 2. Thermolysis of xanthate chain end group of EPVP to form unsaturated chain end. The signal for proton *i* is shown in Figure 2.

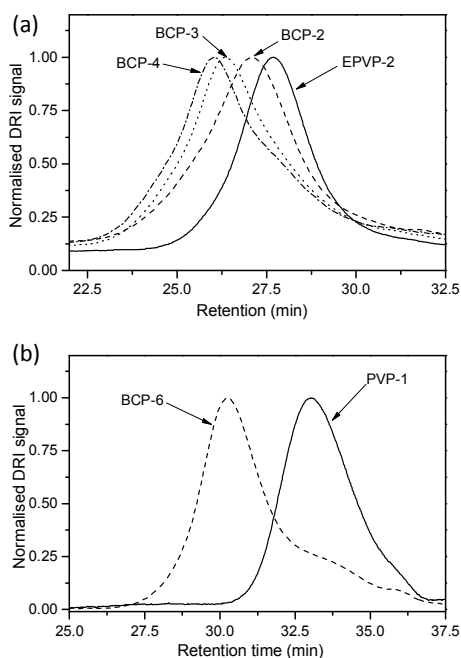


Figure 3. Representative SEC traces of EPVP-PVP (a) and PVP-EPVP (b) BCPs described in Table 2.

BCP-3 showed a sharper change in transmittance as compared to BCP-5 and BCP-6, presumably because BCP-3 has a greater EPVP:PVP (i.e. thermoresponsive:hydrophilic block) ratio than BCP-

5 and BCP-6. This could have influenced the observed transmittance change as reflected in Fig. 5. Various factors such as concentration, molecular weight and copolymerization, which are known to affect the LCST,⁸⁻¹⁰ were also investigated via turbidity measurements. The T_{CP} of EPVP homopolymers was unaffected by polymer molecular weight (Table 3), in agreement with literature reports,³² and the T_{CP}

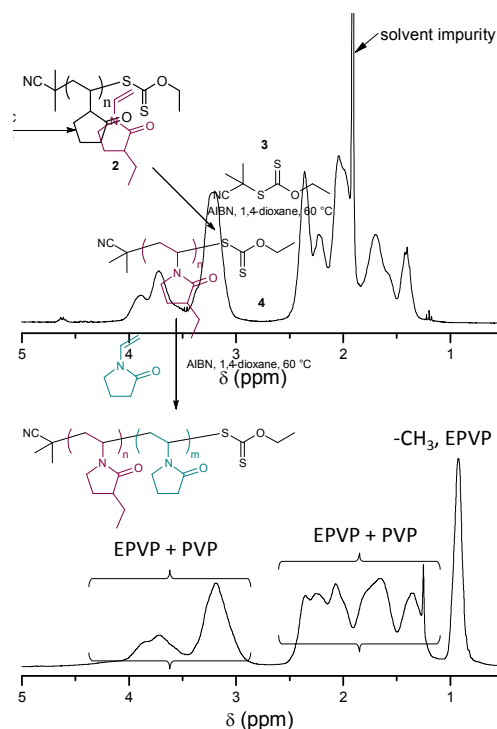


Figure 4. Comparison of ^1H NMR spectra of PVP (top), and the EPVP-PVP block copolymer (bottom) in CDCl_3 , showing EPVP's unique proton signal.

of EPVP-PVP BCPs did not change with increasing concentration in the range of $1.25 - 10 \text{ mg}\cdot\text{mL}^{-1}$ (Fig. 6a). Turbidity measurements of BCPs with a constant thermoresponsive block (EPVP₅₈) length, and varying hydrophilic (PVP) block lengths showed a linear dependency between T_{CP} and hydrophilic block length (Fig. 6b and Table 3). We further examined the thermoresponsive character of the EPVP-PVP BCPs by variable temperature (VT) ^1H NMR spectroscopy in D_2O (Fig. 7). Proton NMR signals of EPVP and PVP overlap extensively, due to their structural similarity, however, EPVP has a unique $-\text{CH}_3$ signal at 0.9 ppm, which we could track unambiguously (see Fig. 4). The EPVP $-\text{CH}_3$ protons signal completely disappeared as the temperature was increased above the LCST due to desolvation of the EPVP block segment (Fig. 7a), which would result in restricting the mobility of EPVP chains. The hydrophilic PVP segments remained solvated, as evidenced by the PVP signals, which remained well resolved at elevated temperatures. This suggested that the BCP was self-assembling, with increasing temperature, with

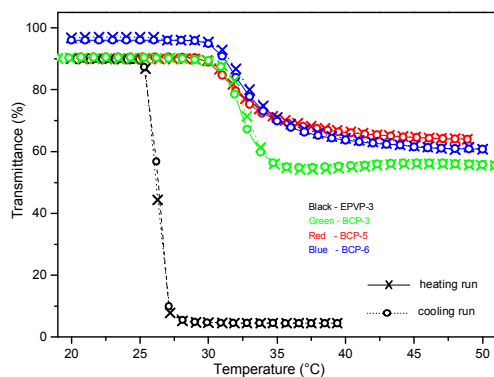


Figure 5. Change in transmittance for single heating and cooling runs for EPVP-3, EPVP-PVP (BCP-5) and PVP-EPVP (BCP-6) thermoresponsive polymers.

Table 3. TCP values of EPVP homopolymers and EPVP-PBP BCs.

| Homopolymer | T_{CP} (°C) | Block copolymer | T_{CP} (°C) |
|------------------|---------------|---|---------------|
| EPVP-1 (DP = 30) | 27.1 | BCP-1 (E-PVP ₃₀ - <i>b</i> -PVP ₆) | 38.5 |
| | | BCP-2 (E-PVP ₅₈ - <i>b</i> -PVP ₂₆) | 30.8 |
| EPVP-2 (DP = 58) | 27.0 | BCP-3 (E-PVP ₅₈ - <i>b</i> -PVP ₃₈) | 32.8 |
| | | BCP-4 (E-PVP ₅₈ - <i>b</i> -PVP ₅₆) | 33.9 |
| EPVP-3 (DP = 90) | 27.2 | BCP-5 (E-PVP ₉₀ - <i>b</i> -PVP ₁₁₆) | 30.1 |

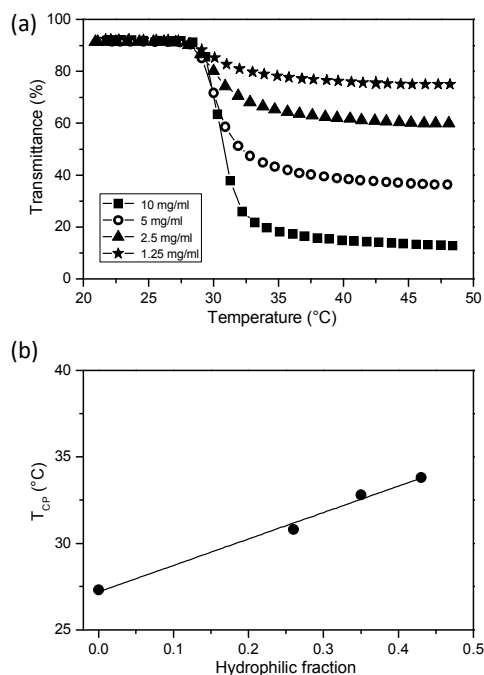


Figure 6. The effect of concentration on the thermoresponsive behaviour of EPVP-PVP, BCP-5, (a) and the plot of the T_{CP} 's of EPVP-2 and EPVP-PVP BCs 2-4 (Table 3) as a function of the hydrophilic mass fraction (f_{NVP}) (b).

the hydrophilic PVP segments shielding the desolvated EPVP segments. The ratio between the integrated signals from the overlapping EPVP and PVP signals, and the unique E-PVP signals

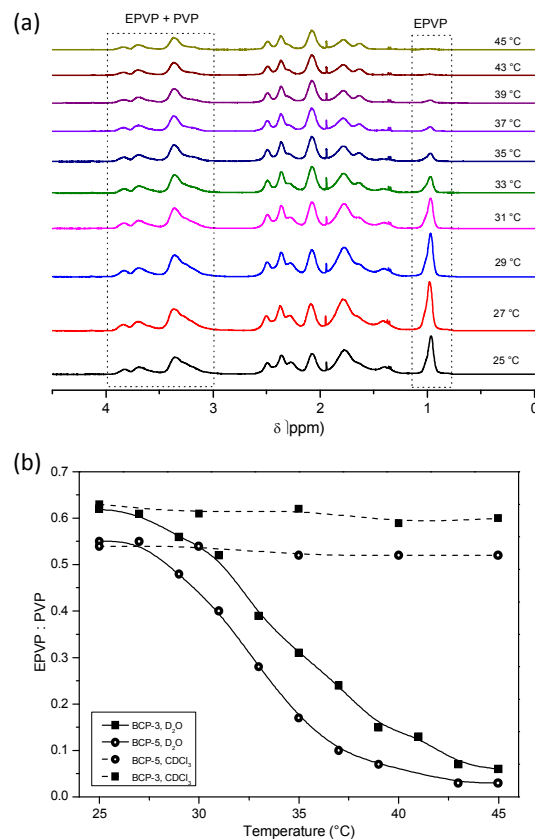


Figure 7. Variable temperature 1H NMR spectra of BCP-3 indicating the $-CH_3$ signals from EPVP and the combined signals from EPVP and PVP (a). A plot of the change in apparent ratio between EPVP and PVP for BCP-3 and BCP-5 as a function of temperature, as calculated from the integrated 1H NMR signals (b).

were then used to determine the apparent EPVP:PVP ratios. The plot of the apparent EPVP:PVP ratios as a function of temperature (Fig 7b) correlated very well with the T_{CP} values of BCP-3 and BCP-5 (see Table 3), obtained from turbidity measurements. For a comparison, BCP samples dissolved in $CDCl_3$, in which the BCP is molecularly dissolved at elevated temperatures, did not show a change in the ratio between EPVP and PVP at elevated temperatures.

Further investigations into the temperature-induced self-assembly of EPVP-PVP were performed using dynamic light scattering (DLS), and cryo-TEM. Unexpectedly, DLS showed the presence of aggregates, of approximately 120 nm, below the T_{CP} . Then at around 27 °C, the hydrodynamic diameter increased drastically, from ~ 120 nm to ~ 200 nm, before decreasing again to ~ 100 nm (Fig. 8, and Fig. S7-S8). Below the LCST, the BCs should exist as molecularly dissolved single polymer chains (unimers) (~ 10 nm), with aggregate formation commencing above the LCST, due to desolvation of the "smart" block segment.^{5-7,9,43} This contrasts our observation of aggregates, of size ~ 120 nm, below the T_{CP} . With the PVP-EPVP BCP-6, however, below the T_{CP} , only aggregates of ~ 10

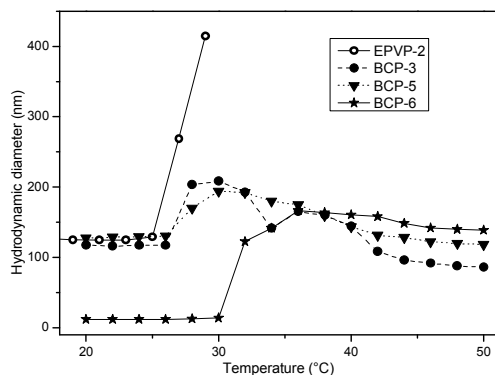


Figure 8. The change in hydrodynamic diameter as a function of temperature for EPVP-PVP (BCP-3 and BCP5), PVP-EPVP (BCP-6) and EPVP-2.

nm were observed (Fig. 8 and Fig. S9), as expected for molecularly dissolved unimers. We also analysed the starting EPVP-2 homopolymer, by DLS and observed that it also contained aggregates of ~ 120 nm below the T_{CP} , similar to EPVP-PVP (Fig. 8). These findings suggest that EPVP, despite its temperature responsive behaviour and the fact that it dissolved in water to give clear homogenous solutions, is not as appreciably hydrophilic, below the T_{CP} , as initially believed.

Further investigations, with cryo-TEM, of the EPVP-PVP BCP prepared from aqueous solutions significantly below the T_{CP} (5 °C, Fig. 9a), revealed the presence of ill-defined aggregates, agreeing with the aggregate formation observed from DLS experiments. This also explained why the percentage transmittance, obtained from turbidity measurements, *vide supra*, started below 100% as aggregates were already present. The EPVP-PVP BCPs used in the study contained EPVP homopolymer impurities, carried over from the EPVP first block synthesis, which could have contributed to aggregate formation observed even below the T_{CP} . It has been reported that homopolymer species can affect BCP self-assembly.⁴⁴ That the PVP-EPVP BCP used also contained PVP first block homopolymer impurity, but did not display aggregate formation below the LCST, merely served to confirm the excellent aqueous solubility of PVP. The final decrease in the hydrodynamic volume, observed as the temperature was further increased above 36 °C, (Fig 8) appears consistent with the dehydration observed for temperature-induced aggregates.^{6,7} We also analysed morphologies of aggregates formed by the smart BCPs using TEM. TEM images acquired from aqueous solutions of EPVP-PVP prepared above the T_{CP} (37 °C) showed the formation of well-defined micellar morphologies (Fig. 9b, and Fig. S10). Closer inspection of the TEM images, however, showed the presence of a significant population of small spherical structures (10-20 nm), alongside larger ones (30-50 nm). It is likely that the small spherical structures in the TEM images were formed from homopolymer impurities, observed as undefined aggregates with cryo-TEM, but appear as defined spherical aggregates in the TEM, due to drying-in effects during sample preparation.

TEM images of PVP-EPVP blocks, from samples prepared above the T_{CP} (37 °C), also displayed the formation of uniformly sized spherical morphologies. Surprisingly, the morphologies formed by the

thermoresponsive PVP-EPVP blocks were concentration dependent (Fig. 9c and e). Aqueous PVP-EPVP solutions prepared at 5 – 8 % solids showed the exclusive formation of spherical micellar

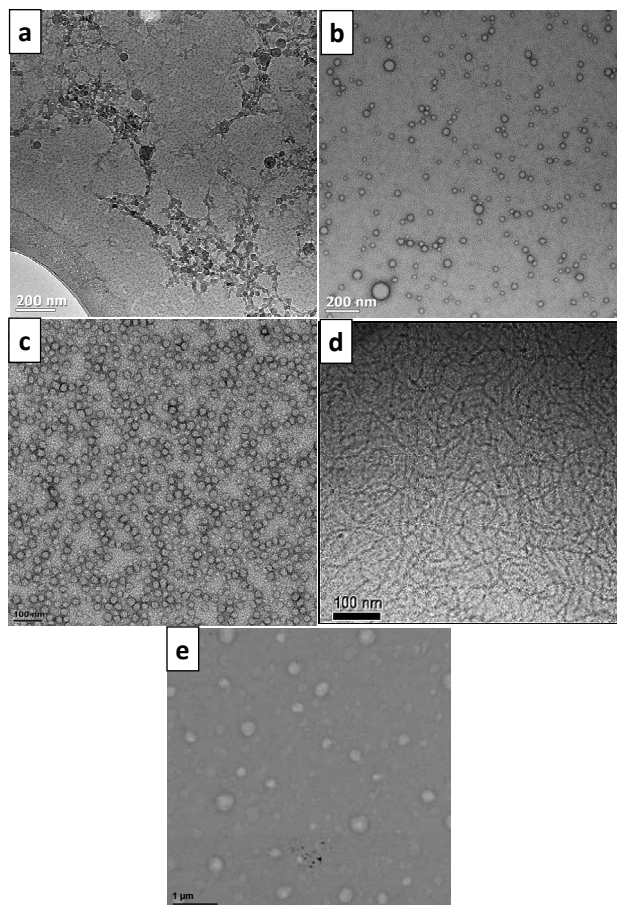


Figure 9. Cryo-TEM image of EPVP-PVP (BCP-3) at 5 °C (a); and TEM images (BCP-3) at 37 °C (b), and the various morphologies formed by aqueous solutions of PVP-EPVP (BCP-6) block copolymers at 7 wt % (c), 11 wt % (d) and 18 wt % (e).

structures. Solutions prepared at 10 – 12 % solids showed the formation of cylindrical micelles. Solutions prepared at 15 – 20 % solids, however, showed the formation of large spherical aggregates which can reasonably be considered to be vesicles. Normally, the concentration dependent formation of multiple morphologies, in dilute solutions, is realised using mixed solvents in which one of the solvents is a non-solvent for one of the block segments of the BCP.⁴⁵⁻⁴⁷ This effect is caused by an increase in the aggregation number, with increasing concentration, thereby causing the morphology to change from spherical to cylindrical micelles and to vesicles.^{3,48,49} This concentration dependant structural evolution of morphologies enhances the versatility of this BCP system, and should make it an attractive target for biomedical applications such as drug delivery.

Conclusions

In conclusion, we have demonstrated a facile synthesis of a well-defined thermoresponsive block copolymer based on EPVP/PVP, using a xanthate mediated RAFT polymerization process. The temperature induced self-assembly was studied using a combination or ^1H NMR spectroscopy, UV-vis spectroscopy, DLS and TEM. We observed that EPVP was appreciably hydrophobic even below its LCST. The sequence of block synthesis could be interchanged, without affecting the control of the polymerization. However, for the self-assembly, it is advantageous to synthesize the PVP block first, because EPVP homopolymer impurities form undefined aggregates which affect the temperature induced self-assembly. On the other hand, PVP homopolymer impurities did not appear to influence the temperature induced self-assembly behaviour of PVP-EPVP blocks.

We observed a concentration dependant morphogenic effect of the thermally induced self-assembly. Aggregates formed by heating aqueous solutions of PVP-EPVP block copolymers, changed from spherical to cylindrical micelles and finally vesicles, as a function of increasing concentration. Both EPVP and PVP are biocompatible, making this block copolymer an excellent addition to known thermoresponsive block copolymer systems, which can be used for advanced drug delivery. Further studies are now focused on assessing the effects of different parameters on morphology and the full phase diagram.

Acknowledgements

The authors acknowledge the support through the South African Research Chairs Initiative (SARChI) from the Department of Science and Technology (DST) and the National Research Foundation (NRF) of South Africa.

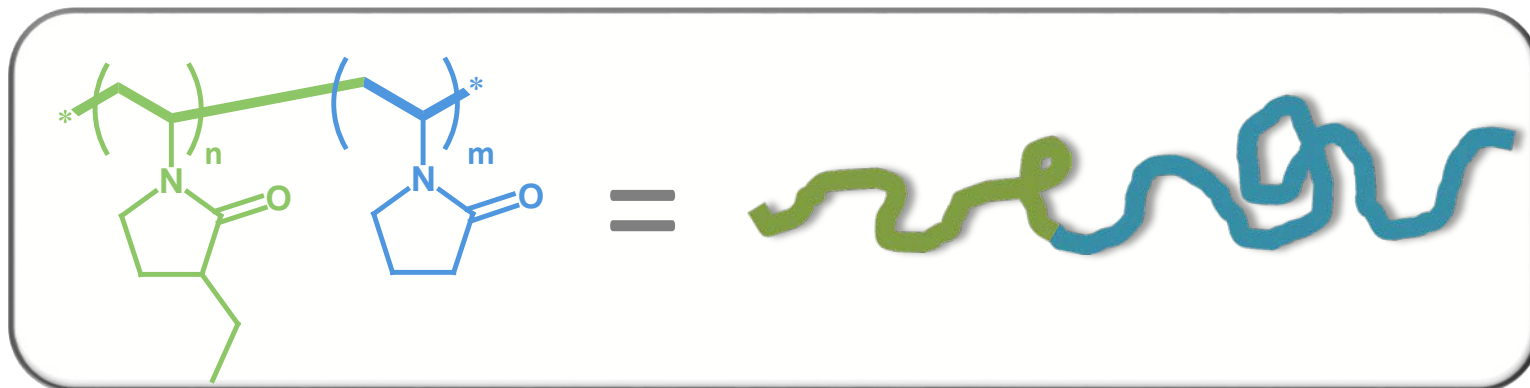
References

- (1) Cabane, E.; Zhang, X.; Langowska, K.; Palivan, C.; Meier, W. *Biointerphases* **2012**, *7*, 1.
- (2) Alarcon, C. d. I. H.; Pennadam, S.; Alexander, C. *Chem. Soc. Rev.* **2005**, *34*, 276.
- (3) Mai, Y.; Eisenberg, A. *Chem. Soc. Rev.* **2012**, *41*, 5969.
- (4) Alexander, C.; Shakesheff, K. M. *Adv. Mater.* **2006**, *18*, 3321.
- (5) Qin, S.; Geng, Y.; Discher, D. E.; Yang, S. *Adv. Mater.* **2006**, *18*, 2905.
- (6) Convertine, A. J.; Lokitz, B. S.; Vasileva, Y.; Myrick, L. J.; Scales, C. W.; Lowe, A. B.; McCormick, C. L. *Macromolecules* **2006**, *39*, 1724.
- (7) Li, Y.; Lokitz, B. S.; McCormick, C. L. *Angew. Chem. Int. Ed.* **2006**, *45*, 5792.
- (8) Tong, Z.; Zeng, F.; Zheng, X.; Sato, T. *Macromolecules* **1999**, *32*, 4488.
- (9) Wang, Y.-C.; Tang, L.-Y.; Li, Y.; Wang, J. *Biomacromolecules* **2009**, *10*, 66.
- (10) Xia, Y.; Yin, X.; Burke, N. A. D.; Stöver, H. D. H. *Macromolecules* **2005**, *38*, 5937.
- (11) Yamamoto, K.; Serizawa, T.; Akashi, M. *Macromol. Chem. Phys.* **2003**, *204*, 1027.
- (12) Zhou, Y.; Yan, D.; Dong, W.; Tian, Y. *J. Phys. Chem. B* **2007**, *111*, 1262.
- (13) De, P.; Sumerlin, B. S. *Macromol. Chem. Phys.* **2013**, *214*, 272.
- (14) Miyazaki, H.; Kataoka, K. *Polymer* **1996**, *37*, 681.
- (15) Meng, F.; Zhong, Z. *J. Phys. Chem. Lett.* **2011**, *2*, 1533.
- (16) Meng, F.; Zhong, Z.; Feijen, J. *Biomacromolecules* **2009**, *10*, 197.
- (17) Li, M.-H.; Keller, P. *Soft Matter* **2009**, *5*, 927.
- (18) Rapoport, N. *Prog. Polym. Sci.* **2007**, *32*, 962.
- (19) Bütün, V.; Armes, S. P.; Billingham, N. C. *Polymer* **2001**, *42*, 5993.
- (20) Weaver, J. V. M.; Bannister, I.; Robinson, K. L.; Bories-Azeau, X.; Armes, S. P.; Smalridge, M.; McKenna, P. *Macromolecules* **2004**, *37*, 2395.
- (21) Lutz, J.-F.; Akdemir, Ö.; Hoth, A. *J. Am. Chem. Soc.* **2006**, *128*, 13046.
- (22) Hu, Z.; Cai, T.; Chi, C. *Soft Matter* **2010**, *6*, 2115.
- (23) Zhang, K.; Khan, A. *Macromolecules* **1995**, *28*, 3807.
- (24) Mortensen, K.; Brown, W.; Joergensen, E. *Macromolecules* **1994**, *27*, 5654.
- (25) Verdonck, B.; Gohy, J.-F.; Khouzakoun, E.; Jérôme, R.; Du Prez, F. *Polymer* **2005**, *46*, 9899.
- (26) Roy, D.; Brooks, W. L. A.; Sumerlin, B. S. *Chem. Soc. Rev.* **2013**, *42*, 7214.
- (27) Trellenkamp, T.; Ritter, H. *Macromol. Rapid Commun.* **2009**, *30*, 1736.
- (28) Lai, H.; Chen, G.; Wu, P.; Li, Z. *Soft Matter* **2012**, *8*, 2662.
- (29) Chen, G.-T.; Wang, C.-H.; Zhang, J.-G.; Wang, Y.; Zhang, R.; Du, F.-S.; Yan, N.; Kou, Y.; Li, Z.-C. *Macromolecules* **2010**, *43*, 9972.
- (30) Hoffman, A. S. *J. Controlled Release* **1987**, *6*, 297.
- (31) Yan, N.; Zhang, J.-g.; Tong, Y.; Yao, S.; Xiao, C.; Li, Z.; Kou, Y. *Chem. Commun.* **2009**, 4423.
- (32) Yan, N.; Zhang, J.; Yuan, Y.; Chen, G.-T.; Dyson, P. J.; Li, Z.-C.; Kou, Y. *Chem. Commun.* **2010**, *46*, 1631.
- (33) Haaf, F.; Sanner, A.; Straub, F. *Polym J* **1985**, *17*, 143.
- (34) Maji, S.; Zhang, Z.; Voorhaar, L.; Pieters, S.; Stubbe, B.; Van Vlierberghe, S.; Dubruel, P.; De Geest, B. G.; Hoogenboom, R. *RSC Adv.* **2015**, *5*, 42388.
- (35) Pakuro, N.; Yakimansky, A.; Chibirova, F.; Arest-Yakubovich, A. *Polymer* **2009**, *50*, 148.
- (36) Salamova, U. U.; Rzaev, Z. M. O.; Altindal, Ş.; Masimov, A. A. *Polymer* **1996**, *37*, 2415.
- (37) Maeda, Y.; Nakamura, T.; Ikeda, I. *Macromolecules* **2002**, *35*, 217.
- (38) Nakhmanovich, B. I.; Pakuro, N. I.; Akhmet'eva, E. I.; Litvinenko, G. I.; Arest-Yakubovich, A. A. *Polym. Sci. Ser. B* **2007**, *49*, 136.
- (39) Keddie, D. J. *Chem. Soc. Rev.* **2014**, *43*, 496.
- (40) Bouhadir, G.; Legrand, N.; Quiclet-Sire, B.; Zard, S. Z. *Tetrahedron Lett.* **1999**, *40*, 277.
- (41) Pound, G.; McLeary, J. B.; McKenzie, J. M.; Lange, R. F. M.; Klumperman, B. *Macromolecules* **2006**, *39*, 7796.
- (42) Pound, G.; Eksteen, Z.; Pfukwa, R.; McKenzie, J. M.; Lange, R. F. M.; Klumperman, B. *J. Polym. Sci., Part A: Polym. Chem.* **2008**, *46*, 6575.
- (43) Pietsch, C.; Mansfeld, U.; Guerrero-Sanchez, C.; Hoepfener, S.; Vollrath, A.; Wagner, M.; Hoogenboom, R.; Saubern, S.; Thang, S. H.; Becer, C. R.; Chiefari, J.; Schubert, U. S. *Macromolecules* **2012**, *45*, 9292.
- (44) Zhang, L.; Eisenberg, A. *J. Am. Chem. Soc.* **1996**, *118*, 3168.
- (45) Zhang, L.; Shen, H.; Eisenberg, A. *Macromolecules* **1997**, *30*, 1001.

Journal Name

ARTICLE

- (46) Zhang, L.; Eisenberg, A. *Macromolecules* **1999**, *32*, 2239.
- (47) Chen, X.; Ding, X.; Zheng, Z.; Peng, Y. *Macromol. Biosci.* **2005**, *5*, 157.
- (48) Zhang, L.; Barlow, R. J.; Eisenberg, A. *Macromolecules* **1995**, *28*, 6055.
- (49) Blanazs, A.; Armes, S. P.; Ryan, A. J. *Macromol. Rapid Commun.* **2009**, *30*, 267.

$< 30\text{ }^{\circ}\text{C}$  $> 37\text{ }^{\circ}\text{C}$ 

Concentration

